FNAS: Uncertainty-Aware Fast Neural Architecture Search

Jihao Liu^{1, 2}, Ming Zhang¹, Yangting Sun¹, Boxiao Liu¹, Yu Liu^{1, 2}, and Hongsheng Li^{2, 3}

¹SenseTime X-Lab ²CUHK - SenseTime Joint Lab, The Chinese University of Hong Kong ³School of CST, Xidian University

Abstract

Reinforcement learning (RL)-based neural architecture search (NAS) generally guarantees better convergence yet suffers from the requirement of huge computational resources compared with gradient-based approaches, due to the rollout bottleneck – exhaustive training of each sampled architecture on the proxy tasks. In this paper, we propose a general pipeline to accelerate the convergence of the rollout process as well as the RL process in NAS. It is motivated by the interesting observation that both the architecture and the parameter knowledge can be transferred between different search processes and even different tasks. We first introduce an uncertainty-aware critic (value function) in Proximal Policy Optimization (PPO) [27] to take advantage of the architecture knowledge in previous search processes, which stabilizes the training process and reduce the searching time by 4 times. In addition, an architecture knowledge pool together with a block similarity function is proposed to utilize parameter knowledge and reduces the searching time by 2 times. To the best of our knowledge, this is the first method that introduces a block-level weight sharing scheme in RL-based NAS. The block similarity function guarantees a 100% hit ratio with strict fairness [5]. Besides, we show that an off-policy correction factor used in "replay buffer" of RL optimization can further reduce half of the searching time. Experiments on the Mobile Neural Architecture Search (MNAS) [30] search space show that the proposed Fast Neural Architecture Search (FNAS) accelerates the standard RL-based NAS process by \sim 10x (e.g., 20,000 GPU hours to 2,000 GPU hours for MNAS), and guarantees better performance on various vision tasks.

1 Introduction

The architecture of a convolutional neural network (CNN) is crucial for many deep learning tasks such as image classification [31] and object detection [32]. The widespread use of neural architecture search (NAS) methods such as differentiable, one-shot, evolutional, and RL-based approaches have effectively dealt with architecture design problems. Despite having high performance due to its sampling-based mechanism [30, 41, 31], RL-based NAS tends to require unbearable computing resources which discourages the research community from exploring it further.

The main obstacles to the propagation of RL-based NAS algorithm come from the following two aspects: a) it's necessary to sample a large number of architectures from the search space to ensure the convergence of the RL agent, b) the inevitable training and evaluation cost of these architecture samples on proxy tasks. For example, the seminal RL-based NAS [40] approach requires 12,800 generations of architectures. The state-of-the-art MNAS [30] and MobileNet-V3 [12] require 8000 or more generations to find the optimal architecture. Coupled with \sim 5 epochs training for each generation, the whole search process costs nearly 64 TPUv2 devices for 96 hours or 20,000 GPU

hours on V100 for just one single searching process. With no access to reduce the unbearable computational cost, RL-based NAS is hard to make more widespread influence than differential [21, 4], and one-shot based [1, 9] methods.

On the contrary, the high efficiency of one-shot NAS family brings it continuous research attention. Instead of sampling a huge number of sub-networks, one-shot NAS assembles them into a single super-network. The parameters are shared between different sub-networks during the training of the super-network. In this way, the training process is condensed from training thousands of sub-networks into training a super-network. However, this weight sharing strategy may cause problems of inaccurate performance estimation of sub-networks. For example, two sub-networks may propagate conflicting gradients to their shared components, which may converge to favor one of the sub-networks and repel the other one randomly. This conflicting phenomenon may result in instability of the search process and inferior final architectures, compared with RL-based methods.

In this work, we aim at combining advantages of both RL-based methods and one-shot methods. The proposed method is based on two important *key observations*: First, the optimal architectures for different tasks have certain common architecture knowledge (similar sub-architectures in different search processes' optimal architectures). Second, the parameter knowledge (weights at samples' training checkpoints) can also be transferred across different searching settings and even tasks.

Based on the two observations, to transfer architecture knowledge, we develop Uncertainty-Aware Critic (UAC) to learn the architecture-performance joint distribution from previous search processes in an unbiased manner, utilizing the transferability of the architecture knowledge, which reduces the needed samples in RL optimization process by 50%. For the transferable parameter knowledge, we propose an Architecture Knowledge Pool (AKP) to restore the block-level [30] parameters and fairly share them as new sample architectures' initialization, which speed up each sample's convergence for \sim 2 times. Finally, we also develop an Architecture Experience Buffer (AEB) with an off-policy correctness factor to store the previously trained models for reusing in RL optimization, with half of the search time saved. Under the same environment as MNAS [30] with MobileNet-v3 [12], FNAS speeds up the search process by $10\times$ and the searched architecture performs even better.

To summarize, our main contributions are as follows:

- 1. We propose FNAS, which introduces three acceleration modules, uncertainty-aware critic, architecture knowledge pool, and architecture experience buffer, to speed up reinforcement-learning-based neural architecture search by $\sim 10 \times$.
- 2. We show that the knowledge of neural architecture search processes can be transferred, which is utilized to improve sample efficiency of reinforcement learning agent process and training efficiency of each sampled architecture.
- 3. We demonstrate new state-of-the-art accuracy on ImageNet classification, face recognition, and COCO object detection with comparable computational constraints.

2 Related Works

From the perspective of how to estimation the performance of architectures, NAS methods can be classified into two categories, sampling-based and weight-sharing-based methods.

Sampling-based methods generally sample a large number of architectures from the architecture search space and train them independently. Based on the evaluated performance of the well-trained sampled architectures, multiple approaches can be utilized to identify the best-performing one, including Bayesian optimization [14], evolutionary algorithm [25], and optimization of an RL agent [40]. The main drawback of this type of methods is their tremendous time and computational consumption on training the sampled architectures. To alleviate this issue, a common practice is to shorten the training epochs and use proxy networks with fewer filters and cells [41, 30]. Besides, Liu *et al.* [20] proposed to train a network to predict the final performance. We also aim to reduce the training cost, by leveraging the accumulated architecture knowledge and parameter knowledge to accelerate the searching process.

Instead of training many architectures independently, the second type of methods resort to training a super-network and estimate the performance of architectures with shared weights from the supernetwork [1, 34, 21, 4, 36, 3, 29, 9]. With the easy access to performance estimation of each

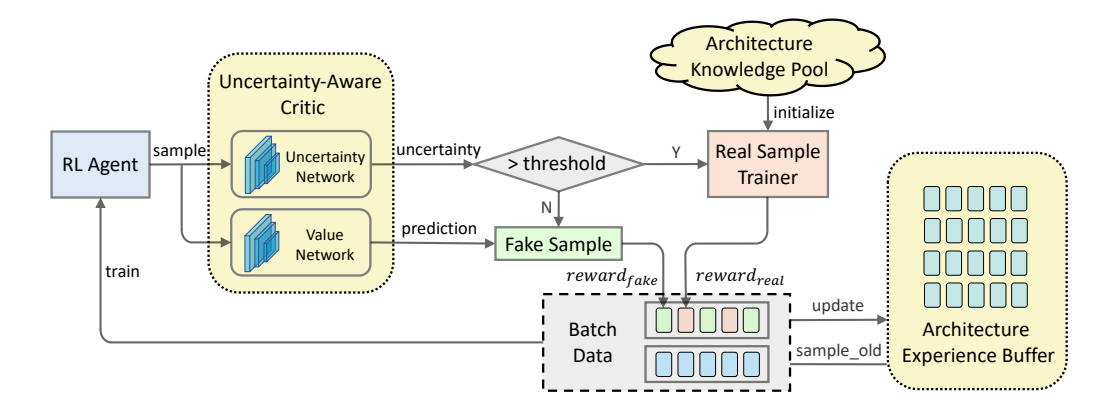


Figure 1: The pipeline of FNAS. The proposed modules are highlighted in orange. Architectures are sampled by the RL agent and then passed to Uncertainty-Aware Critic (UAC) for predicting performance and the corresponding uncertainty. Then a decision module will determine whether the sample needs to be trained by Trainer. The Architecture Knowledge Pool (AKP) helps to initialize new samples for training. Half of the samples in one batch come from Architecture Experience Buffer (AEB), the other half come from Trainer or UAC's Value Network.

sub-architecture, DARTS [21] introduced a gradient-based method to search for the best architecture in an end-to-end manner. However, as pointed in [17], the estimated architecture performances based on weight-sharing networks might be unreliable. Chen *et al.* [4] proposed to progressively shrink the search space so that the estimation can be gradually more accurate. Cai *et al.* [3] introduced a shrinking based method to train the super-network so as to generate networks of different scales without re-training.

Besides, some existing works have tried to combine these two types of methods and reserve both of their advantages [28, 39]. BONAS, introduced in [28], is a sampling-based algorithm that utilizes weight-sharing to evaluate a batch of architectures simultaneously, which reduces the training cost significantly. Although weight-sharing in a batch can make the training more fair, the sub-networks in a batch are selected based on Bayesian Optimization method and can interfere each other in the training process, making the estimate of performance unreliable. Zhao *et al.* [39] propose to use multiple super-networks to alleviate the undesired co-adaption, which is highly sensitive to the splitting strategy of the search space. Cai *et al.* [2] propose to transform the architecture repeatedly in the search process, where the weight of network can be reused to save computational cost. In our pipeline, we also propose to share weights between architectures but in a different way. We construct a general weight pool with many trained architectures. Whenever a new architecture is trained, we initialize the architecture by the trained architectures in the pool. In this way, the number of training epochs for the new architecture can be reduced without harming the reliability of performance estimation Figure 3c.

3 Preliminary Observation

RL-based NAS generally consumes quite expensive computing resources. MNAS [30] needs to train 8,000 models for training its RL agent until convergence, which costs 20,000 GPU hours on V100. Each architecture sample trained for one NAS process would not be used again. However, state-of-the-art differentiable-based NAS [21, 35, 4, 34] demonstrated that, with various weight-sharing techniques, the NAS algorithms can be significantly accelerated. In this section, we will show that the knowledge of previous searched processes can be reused, which can accelerate the NAS processes.

3.1 Architecture knowledge can be transferred

Optimal architectures for different tasks have common architecture knowledge. It can be observed in many applications that a good network architecture in one task tends to generalize to work well on other tasks. An illustrative example of the observation is adopting the pre-trained ImageNet

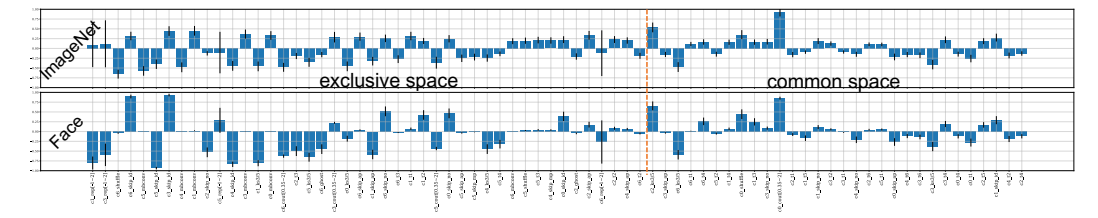


Figure 2: Expectation of each operator of optimal models of face and ImageNet architecture search processes. Calculated by the 100 optimal models of face and ImageNet architecture search processes and sorted by the significance of the difference.

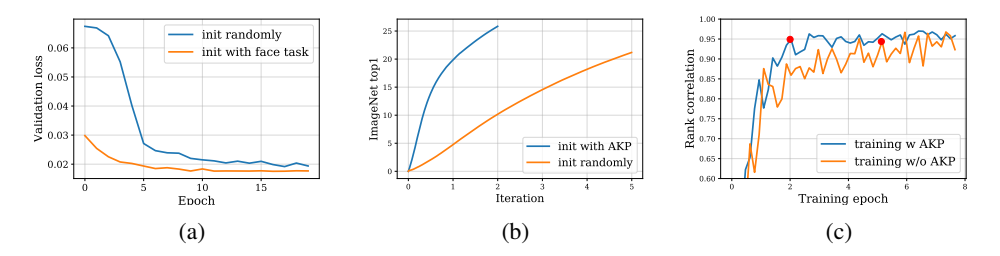


Figure 3: On the left, the value function pretrained on face recognition tasks converges much faster. On the right, Spearman rank-order correlation [38] along the training process of random initialization and block-level initialization.

[6] models as the backbone networks for object detection [19], semantic segmentation [18], face recognition [7], etc. In NAS, however, this assumption needs to be carefully verified as there exist a huge search space of network architectures Here, We statistically verify whether this observation also holds for NAS.

In Figure 2, we sample 100 optimal architectures of one face recognition search process and one ImageNet classification search process, respectively. For each architecture, we firstly expand its tokens to one-hot representation following [22]. After that, we can compare statistical divergence between the architecture family of face and ImageNet search processes. The results are shown in Figure 2. Similar conclusions can be obtained that the operators can be divided into two categories, one with large differences and the other with small differences.

Many previous works [20, 16, 24, 33, 23] use a predictor to predict an architecture's performance to speed up the NAS process. However, as the predictor requires thousands of samples to train, they usually evolves in a progressive [20] or semi-supervised manner [23]. Inspired by the interesting observation above, we implement it in a unified way where different search processes' samples are used together to train a unified value network to map each architecture's one-hot representation [22] to its performance. When running a new search experiment, we just use directly the unified network trained by the old data and keep updating it in the new task during the search process, which speeds up the convergence of the value network. As shown in Figure 3a, when transferring a value network trained on ImageNet to face recognition task, the network converges much faster.

3.2 Parameter knowledge can be transferred

Initializing the network by ImageNet pre-trained models and training the model on other tasks has generally been a standard way as it can speed up the convergence process. However, pretraining has been ignored in NAS as it may break the rank orders of different models. In our experiments, we observe that the parameter knowledge can help us to obtain the accurate rank correlations faster than training from scratch. Besides, this property holds regardless of the data distribution. We randomly sample 50 models and train them on ImageNet in two ways: from scratch or by initializing with parameter knowledge from face recognition models. Then, we compare the rank order of validation set performance with the actual rank (i.e. fully trained rank) along the training process. As shown in

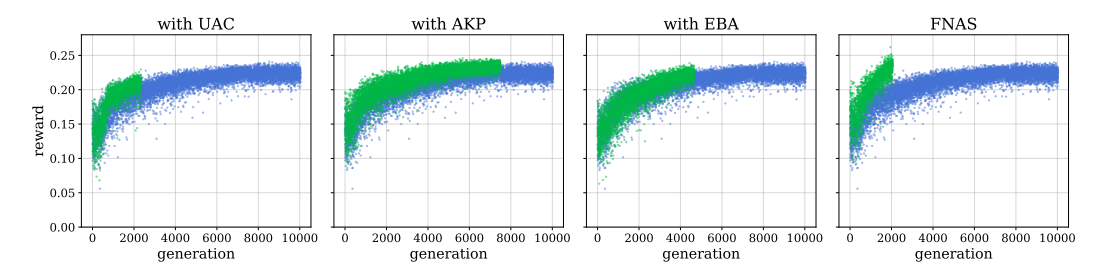


Figure 4: Reward along sample generation between FNAS and MNAS. Blue dots are the searching result of MNAS, while green dots are the results of FNAS.

Figures 3b and 3c, with *parameter knowledge* from face recognition models, we can obtain more accurate rank in fewer epochs.

4 Uncertainty-Aware Neural Architecture Search

In this section, we introduce how we utilize the observations above to design three core modules to inherit common architecture knowledge and parameter knowledge from other tasks.

4.1 Architecture search with Reinforcement Learning

Following [30, 41], we use Proximal Policy Optimization (PPO) [27] to find our Pareto optimal solutions for our multi-objective search problem. Concretely, we follow the same idea as [30, 41] and map each sample architecture in the search space to a list of tokens. These tokens are determined by a sequence of actions $a_{1:T}$ from the RL agent with policy π_{θ} . Our goal is to maximize the expected reward

$$\mathbb{J} = \mathbb{E}_{P_{(a_{1:T};m)}} R(m) \tag{1}$$

where m is a sampled model determined by action $a_{1:T}$, and R(m) is the reward of m. We use the same definition of R(m) of [30] for fair comparison

$$R(m) = ACC(m) \times \left\lceil \frac{LAT(m)}{T} \right\rceil^{\alpha}, \tag{2}$$

where ACC(m) is the accuracy on the proxy task, LAT(m) is the latency on target hardware, T is the target latency, and α is the weight factor.

Following [30], we use a well known sample-eval-update loop to update the policy π_{θ} . At each iteration, π_{θ} firstly generates a batch of samples by predicting a sequence of tokens with its LSTM. For each sample m, we train it on the proxy task to obtain ACC(m) and run it on target hardware to obtain LAT(m). R(m) is calculated with Eq. (2). We then update the policy π_{θ} to maximize the expected reward (Eq. (1)) using PPO.

4.2 Uncertainty-Aware Critic in Proximal Policy Optimization (PPO)

The value function is a common module and is widely used in RL algorithms such as PPO but rarely used in traditional NAS. Usually, training a value function requires a large number of samples (e.g., million-level steps in Atari environment trained by ray¹), which is unbearable for NAS as it is equivalent to training thousands of models needed to be trained and it's expensive. In our algorithm, we propose the Uncertainty-Aware Critic (UAC) to deal with this issue, which is inspired by our observations as mentioned in Section 3.

Given an architecture m sampled from the search space, a value network V is utilized to predict the reward V(m) of this sample, while R(m) is the actual reward of it. The loss function to update V is

¹https://github.com/ray-project/rl-experiments

formulated as

$$L_V = |V(m) - R(m)| \tag{3}$$

Besides, an uncertainty network U is utilized to predict the uncertainty U(m) of this sampled architecture m, which is used to learn discriminately whether a sample is in the distribution of learned samples. The loss function to supervise U is formulated as

$$L_U = |U(m) - L_V| \tag{4}$$

If U(m) is greater than a threshold, the sample may locate in an untrusted region, which indicates that the sampled architecture m has not been effectively learned by the value network. As a result, it would be trained on a proxy task from scratch to get its reward R(m). Otherwise, it can be assumed that the prediction V(m) is accurate, and V(m) would be regarded as R(m) to update the RL agent. The threshold is set to ensure 2 times speedup while avoiding the risk of over-fitting. The whole process is illustrated in Figure 1.

Samples that need to be trained from scratch are named as untrusted samples, while the remaining ones whose reward comes from V are named as trusted samples. With more untrusted samples obtaining their rewards along the search process, the value network becomes more accurate, thus the uncertainty predicted by U gradually decreases. Considering an extreme case, where each sample in a batch obtains a reward with low uncertainty and is classified as trusted sample, the agent trained with these samples is likely to overfit, which is not conducive to the exploration of the RL agent and would lead to inferior performance. In our implementation, we use the following constraint to balance the exploration and the exploitation of the RL agent to speed up its convergence without over-fitting.

• Constraint: In each batch, when the number of trusted samples is greater than 50% of the batch size, the extra trusted samples would be thrown away and the architectures would be resampled until enough untrusted samples are obtained to fill the batch.

With the above constraint, the algorithm can get a decent performance with accelerated search, and the result is shown in Figure 4 (with UAC).

4.3 Uncertainty-Aware Architecture Knowledge Pool

Parameter knowledge can be transferred among different tasks to speed up the convergence of the training process of the sampled architectures as shown in Section 3.2. However, traditional pretrain is not feasible in NAS, as there are thousands of different architectures in the search space and we can not afford to pretrain each architecture on a different task. To address this problem, we propose to initialize each architecture in a factorized way and use a fuzzy matching algorithm to guarantee the hit ratio, which is defined as the division between the number of matched blocks and total queried blocks.

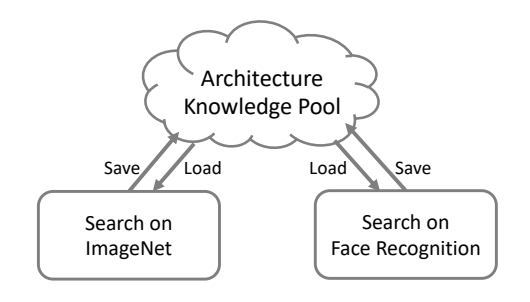


Figure 5: Different tasks share the same global knowledge pool.

Following [30], we define an architecture as a combination of n blocks $\{b_1, b_2, \ldots, b_n\}$.

For any two architectures m_i and m_j , although generally, their structures might be quite different, some of their blocks are similar to each other, (e.g., b_2 of $m_i == b_2$ of m_j), thus the weights of these parts could be shared. So we build a Architecture Knowledge Pool (AKP) to store all the previously trained models' blocks in a key-value table, where the key is the expand embedding [22] of each block and the value is the *Parameter knowledge* of the block.

Recent research has found that fairness in weight sharing has great influence on the final performance of searched architecture [5]. So we apply the following two strategies to solve the problem of fairness.

- The checkpoints stored in the AKP are trained with equal iterations.
- For each block query, the proposed uncertainty function is used to ensure that the match ratio reaches more than 99%, which means less than 1% blocks have been unfairly initialized.

Given a query block b_i , we calculate the cosine similarity of the expanded embedding as in Section 3.1 between b_i and each element in AKP. The block with the highest similarity would be retrieved to initialize b_i . We show the overall process in Figure 5. Our experiments shows that using AKP created from multiple tasks can speed up the search process by $2 \times$ (Figure 3c), as shown in Figure 4 (with AKP).

5 Architecture Experience Buffer (3AEB)

In a general RL task, there are a lot of discussions about sample reuses. However, in RL-based NAS, improving sampling efficiency is rarely investigated. In our algorithm, we propose an architecture experience buffer to store the sampled architectures in the form of architecture-performance pairs, and for each iteration in the future, the stored samples may be used again to update the RL agent to speed up its convergence. We call the samples stored in the experience buffer as exploited sample and the newly generated samples as exploring samples. Different from the traditional RL works, the proposed experience buffer has the following features:

- The buffer size is relatively small (usually 10 in our experiments). As the convergence of the RL agent is much faster than RL tasks, if the buffer size is set too large, the agent will focus on exploited samples and the convergence speed would be slow.
- In each batch, both exploited samples and exploring samples would be selected. To prevent the RL updating from biasing to the exploited samples, the percentage of the exploited samples in one batch is constrained to no more than 50%.

Some recent works [26] suggested that the samples of different properties should be selected in the buffer. We follow the strategy by choosing samples with different reward values. Then, we sample from the buffer and reweight the samples according to their priorities as defined below. For each sample $\{s_1, s_2, \ldots, s_n\}$ with their rewards $R\{r_1, r_2, \ldots, r_n\}$ in AEB, their priority scores are defined as

$$P_i = \frac{exp(r_i)}{\sum_j exp(r_j)} \tag{5}$$

Following [26], each sample would also be reweighted by their importance sampling weights. The reweighted priority scores S can be written as $S_i = (N \cdot P_i)^{-\beta}$, where N is the buffer size and β is the annealing coefficient and would be increased from 0 to 1 as the search proceeds. And the result is shown in Figure 4 (with AEB).

6 Fast Neural Architecture Search (FNAS) on vision tasks

In this section, we conduct different experiments on both ImageNet and million-level face recognition tasks to verify the effectiveness of FNAS. The details and results are as follows:

6.1 Implementation details

Following the standard searching algorithm as NASNet [41], MNAS [30] and AKD [22], we use an RNN-based agent optimized by PPO algorithm [27]. The RL agent is implemented with a one-layer LSTM [11] with 100 hidden units at each layer. The V and U of UAC are implemented with four-layer MLP with 200 hidden units at each layer and PReLU [10] nonlinearity.

For ImageNet experiments, we sample 50K images from the training set to form the mini-val set and use the rest as the mini-training set. In each experiment, 8K models are sampled to update the RL agent. Note that when equipped with UAC or AEB, not all samples need to be activated, as many samples' rewards are directly returned from these two modules. For face experiments, we use MS1M [8] as the mini-training set, LFW [13] as the mini-val set. The final performance is evaluated on MegaFace [15].

Table 1: Performance Results on ImageNet Classification. FNAS-Image×1.3 means scale up FNAS-Image for 1.3× along width.

models	Туре	Mult-Adds	Top1 Acc. (%)	Top5 Acc. (%)	Search Cost (GPU Hours)
MBv2	Manual	300M	72	91	0
ProxylessNAS DARTS FairNAS Once-For-All	Share-weight	320M 574M 388M 327M	74.6 73.3 75.3 75.3	92.2 91.3 92.4 92.6	200 96 288 1200
AmoebaNet	Evolutionary	555M	74.5	92	75,600
MNAS NASNet MBv3 EfficientNetB0 FNAS-Image FNAS-Image×1.3	RL-based	315M 564M 219M 390M 225M 392M	75.2 74 75.2 76.3 75.5 77.2	92.5 91.6 91 93.2 92.6 93.5	20,000 43,200 - 2000 2000

Table 2: Performance on MegaFace.

Table 3: Performance on COCO.

model	Mult-Adds	Distract 1e5	tor num 1e6	Search Cost (GPU Hours)
MBv2	300M	92.75	88.71	0
ShuffleNet	295M	94.15	90.46	0
MNAS	313M	93.41	89.47	20,000
MBv3	218M	94.15	90.64	-
FNAS-Face	227M	95.45	92.63	2000

models	Mult-Adds	mAP
MNAS	13.4 G	27.68
$MBv2\times1.0$	13.3 G	29.79
$MBv3 \times 0.75$	5.852 G	29.25
$MBv3 \times 1.0$	9.060 G	30.02
FNAS	8.021 G	30.44

6.2 Proxyless FNAS on ImageNet

Just as MNAS [30] has done, we also use a multi-objective reward to directly search on ImageNet. After the search process, we retrain the top 10 models with the largest reward near the target Mult-Adds from scratch to verify the search results. In Table 1, we get a relatively higher result than the current SOTA network MBv3 [12]. Note that the model we search does not go through the pruning operation NetAdapt [37], which can reduce $10\%\sim15\%$ computation and keep performance nearly unchanged. Compared with EfficientNetB0 [31], FNAS improves top 1 accuracy by 1 point under comparable computation budget. And still, there is nearly $10\times$ of acceleration in the entire search process compared to MNAS [30] or MBv3 [12].

6.3 Proxyless FNAS on fine-grained facial recognition

Besides verifying the performance of FNAS on ImageNet, we also test it on the fine-grained facial recognition task. As can be seen in Table 2, compared with MBv3, verification accuracy improves 2 points in comparable Mult-Adds under 1e6 distractors. When compared with MBv2, FNAS improves verification accuracy for nearly 4 points with 24% Mult-Adds reduction. The result shows: 1) FNAS has an obvious acceleration effect on different tasks and 2) the importance of searching directly on the target task.

6.4 Transferability on object detection

We combine the model found on ImageNet in Table 1 with the latest pipeline of detection to verify its generalization. Table 3 shows the performance of the model on COCO [19]. It can be seen that compared to MBv3, there is a significant improvement with our searched model.

Table 4: The effectiveness of the three proposed modules, $MBv2 \times 0.38$ means scale up MBv2 for $0.38 \times$ along width

Models	AKP	UAC	AEB	Mult-Adds	Top1 Acc. (%)	Activated Samples	Search Epoches	Search Cost (GPU Hours)
MBv2×0.38				81M	62.65	0	0	0
MNAS				72M 74M	64.23 65.19	8,000 10,000	1 4	4,000 20,000
FNAS	1	√ √	<i>y</i>	75M 76M 72M 72M 85M	64.97 65.22 64.28 64.44 66.25	8,000 8,000 2,300 4,500 2,000	1 2 1 1 1	4,000 10,000 1,150 2,250 1,000

Table 5: Transferability of UAC and AKP

models	UAC or AKP	Mult-Adds	Top1 Acc. (%)	Activated Samples	Search Epoches	Search Cost (GPU Hours)
MNAS	X	181M	73.25	8,000	4	16,000
FNAS	UAC init with face exp	153M	73.91	2,000	4	4,000
MNAS	x	285M	74.62	8,000	4	16,000
FNAS	AKP init with face exp	292M	75.22	4,000	4	8,000

7 Ablation study

7.1 The effectiveness of the three proposed modules.

In this section, the effectiveness of Uncertainty-Aware Critic (UAC), Architecture Knowledge Pool (AKP), Architecture Experience Buffer (AEB) is verified when they are used alone or combined. Details are shown in Table 4. Three conclusions can be observed: 1. Sampling with AKP initialization gets real rank faster; 2. Fewer samples are required when NAS is equipped with UAC and AEB; and $3.10\times$ speedup can be achieved when NAS is equipped with AKP, UAC, and AEB.

7.2 The transferability of the proposed modules.

In Section 3, we mentioned that knowledge between NAS processes is transferable, which is also verified in the experiment. We use the UAC trained on the face as a pre-trained model and then transfer it to the ImageNet architecture search process. In the absence of 3/4 of activated samples, the optimal model surpasses baseline by 0.67% with fewer Mult-Adds, showing in Table 5. In addition, we use AKP with the checkpoints from face architecture search process and then search on ImageNet. In the absence of 1/2 activated samples, performance increases by 0.6%.

8 Conclusion

This paper proposes three modules (UAC, AKP, AEB) to speed up the entire running process of RL-based NAS, which consumes large amounts of computing power before. With these modules, fewer samples and less training computing resources are needed, making the overall search process $10 \times$ faster. We also show the effectiveness of applying those modules on different tasks such as ImageNet, face recognition, and object detection. More importantly, the transferability of UAC and AKP is being tested by our observation and experiments, which will guide us in tapping the knowledge of the NAS process.

References

[1] Gabriel Bender. Understanding and simplifying one-shot architecture search. 2019.

- [2] Han Cai, Tianyao Chen, Weinan Zhang, Yong Yu, and Jun Wang. Efficient architecture search by network transformation. In *Proceedings of the AAAI Conference on Artificial Intelligence*, volume 32, 2018.
- [3] Han Cai, Chuang Gan, and Song Han. Once for all: Train one network and specialize it for efficient deployment. *arXiv preprint arXiv:1908.09791*, 2019.
- [4] Xin Chen, Lingxi Xie, Jun Wu, and Qi Tian. Progressive differentiable architecture search: Bridging the depth gap between search and evaluation. In *Proceedings of the IEEE International Conference on Computer Vision*, pages 1294–1303, 2019.
- [5] Xiangxiang Chu, Bo Zhang, Ruijun Xu, and Jixiang Li. Fairnas: Rethinking evaluation fairness of weight sharing neural architecture search. *arXiv preprint arXiv:1907.01845*, 2019.
- [6] Jia Deng, Wei Dong, Richard Socher, Li-Jia Li, Kai Li, and Li Fei-Fei. Imagenet: A large-scale hierarchical image database. In 2009 IEEE conference on computer vision and pattern recognition, pages 248–255. Ieee, 2009.
- [7] Jiankang Deng, Jia Guo, Niannan Xue, and Stefanos Zafeiriou. Arcface: Additive angular margin loss for deep face recognition. In *Proceedings of the IEEE Conference on Computer Vision and Pattern Recognition*, pages 4690–4699, 2019.
- [8] Yandong Guo, Lei Zhang, Yuxiao Hu, Xiaodong He, and Jianfeng Gao. Ms-celeb-1m: A dataset and benchmark for large-scale face recognition. In *European conference on computer vision*, pages 87–102. Springer, 2016.
- [9] Zichao Guo, Xiangyu Zhang, Haoyuan Mu, Wen Heng, Zechun Liu, Yichen Wei, and Jian Sun. Single path one-shot neural architecture search with uniform sampling. *arXiv preprint arXiv:1904.00420*, 2019.
- [10] Kaiming He, Xiangyu Zhang, Shaoqing Ren, and Jian Sun. Delving deep into rectifiers: Surpassing human-level performance on imagenet classification. In *Proceedings of the IEEE international conference on computer vision*, pages 1026–1034, 2015.
- [11] Sepp Hochreiter and Jürgen Schmidhuber. Long short-term memory. *Neural computation*, 9(8):1735–1780, 1997
- [12] Andrew Howard, Mark Sandler, Grace Chu, Liang-Chieh Chen, Bo Chen, Mingxing Tan, Weijun Wang, Yukun Zhu, Ruoming Pang, Vijay Vasudevan, et al. Searching for mobilenetv3. In *Proceedings of the IEEE International Conference on Computer Vision*, pages 1314–1324, 2019.
- [13] Gary B Huang, Marwan Mattar, Tamara Berg, and Eric Learned-Miller. Labeled faces in the wild: A database forstudying face recognition in unconstrained environments. 2008.
- [14] Kirthevasan Kandasamy, Willie Neiswanger, Jeff Schneider, Barnabas Poczos, and Eric P Xing. Neural architecture search with bayesian optimisation and optimal transport. In *Advances in Neural Information Processing Systems*, pages 2016–2025, 2018.
- [15] Ira Kemelmacher-Shlizerman, Steven M Seitz, Daniel Miller, and Evan Brossard. The megaface benchmark: 1 million faces for recognition at scale. In *Proceedings of the IEEE conference on computer vision and pattern recognition*, pages 4873–4882, 2016.
- [16] Efi Kokiopoulou, Anja Hauth, Luciano Sbaiz, Andrea Gesmundo, Gabor Bartok, and Jesse Berent. Fast task-aware architecture inference. *arXiv preprint arXiv:1902.05781*, 2019.
- [17] Liam Li and Ameet Talwalkar. Random search and reproducibility for neural architecture search. *arXiv* preprint arXiv:1902.07638, 2019.
- [18] Guosheng Lin, Anton Milan, Chunhua Shen, and Ian Reid. Refinenet: Multi-path refinement networks for high-resolution semantic segmentation. In *Proceedings of the IEEE conference on computer vision and pattern recognition*, pages 1925–1934, 2017.
 [19] Tsung-Yi Lin, Michael Maire, Serge Belongie, James Hays, Pietro Perona, Deva Ramanan, Piotr Dollár,
- [19] Tsung-Yi Lin, Michael Maire, Serge Belongie, James Hays, Pietro Perona, Deva Ramanan, Piotr Dollár, and C Lawrence Zitnick. Microsoft coco: Common objects in context. In European conference on computer vision, pages 740–755. Springer, 2014.
- [20] Chenxi Liu, Barret Zoph, Maxim Neumann, Jonathon Shlens, Wei Hua, Li-Jia Li, Li Fei-Fei, Alan Yuille, Jonathan Huang, and Kevin Murphy. Progressive neural architecture search. In *Proceedings of the European Conference on Computer Vision (ECCV)*, pages 19–34, 2018.
- [21] Hanxiao Liu, Karen Simonyan, and Yiming Yang. Darts: Differentiable architecture search. *arXiv preprint arXiv:1806.09055*, 2018.
- [22] Yu Liu, Xuhui Jia, Mingxing Tan, Raviteja Vemulapalli, Yukun Zhu, Bradley Green, and Xiaogang Wang. Search to distill: Pearls are everywhere but not the eyes. arXiv preprint arXiv:1911.09074, 2019.
- [23] Renqian Luo, Xu Tan, Rui Wang, Tao Qin, Enhong Chen, and Tie-Yan Liu. Semi-supervised neural architecture search. *arXiv preprint arXiv:2002.10389*, 2020.
- [24] Renqian Luo, Fei Tian, Tao Qin, Enhong Chen, and Tie-Yan Liu. Neural architecture optimization. In *Advances in neural information processing systems*, pages 7816–7827, 2018.
- [25] Esteban Real, Alok Aggarwal, Yanping Huang, and Quoc V Le. Regularized evolution for image classifier architecture search. In *Proceedings of the aaai conference on artificial intelligence*, volume 33, pages 4780–4789, 2019.
- [26] Tom Schaul, John Quan, Ioannis Antonoglou, and David Silver. Prioritized experience replay. arXiv preprint arXiv:1511.05952, 2015.
- [27] John Schulman, Filip Wolski, Prafulla Dhariwal, Alec Radford, and Oleg Klimov. Proximal policy optimization algorithms. *arXiv preprint arXiv:1707.06347*, 2017.
- [28] Han Shi, Renjie Pi, Hang Xu, Zhenguo Li, James T Kwok, and Tong Zhang. Bridging the gap between sample-based and one-shot neural architecture search with bonas. arXiv preprint arXiv:1911.09336, 2019.

- [29] Dimitrios Stamoulis, Ruizhou Ding, Di Wang, Dimitrios Lymberopoulos, Bodhi Priyantha, Jie Liu, and Diana Marculescu. Single-path nas: Designing hardware-efficient convnets in less than 4 hours. arXiv preprint arXiv:1904.02877, 2019.
- [30] Mingxing Tan, Bo Chen, Ruoming Pang, Vijay Vasudevan, Mark Sandler, Andrew Howard, and Quoc V Le. Mnasnet: Platform-aware neural architecture search for mobile. In *Proceedings of the IEEE Conference on Computer Vision and Pattern Recognition*, pages 2820–2828, 2019.
- [31] Mingxing Tan and Quoc V Le. Efficientnet: Rethinking model scaling for convolutional neural networks. *arXiv preprint arXiv:1905.11946*, 2019.
- [32] Mingxing Tan, Ruoming Pang, and Quoc V Le. Efficientdet: Scalable and efficient object detection. arXiv preprint arXiv:1911.09070, 2019.
 [33] Wei Wen, Hanxiao Liu, Hai Li, Yiran Chen, Gabriel Bender, and Pieter-Jan Kindermans. Neural predictor
- [33] Wei Wen, Hanxiao Liu, Hai Li, Yiran Chen, Gabriel Bender, and Pieter-Jan Kindermans. Neural predictor for neural architecture search. arXiv preprint arXiv:1912.00848, 2019.
- [34] Bichen Wu, Xiaoliang Dai, Peizhao Zhang, Yanghan Wang, Fei Sun, Yiming Wu, Yuandong Tian, Peter Vajda, Yangqing Jia, and Kurt Keutzer. Fbnet: Hardware-aware efficient convnet design via differentiable neural architecture search. In *Proceedings of the IEEE Conference on Computer Vision and Pattern Recognition*, pages 10734–10742, 2019.
- [35] Sirui Xie, Hehui Zheng, Chunxiao Liu, and Liang Lin. Snas: stochastic neural architecture search. *arXiv* preprint arXiv:1812.09926, 2018.
- [36] Yuhui Xu, Lingxi Xie, Xiaopeng Zhang, Xin Chen, Guo-Jun Qi, Qi Tian, and Hongkai Xiong. Pc-darts: Partial channel connections for memory-efficient architecture search. In *International Conference on Learning Representations*, 2019.
- [37] Tien-Ju Yang, Andrew Howard, Bo Chen, Xiao Zhang, Alec Go, Mark Sandler, Vivienne Sze, and Hartwig Adam. Netadapt: Platform-aware neural network adaptation for mobile applications. In *Proceedings of the European Conference on Computer Vision (ECCV)*, pages 285–300, 2018.
- [38] Jerrold H Zar. Spearman rank correlation. Encyclopedia of Biostatistics, 7, 2005.
- [39] Yiyang Zhao, Linnan Wang, Yuandong Tian, Rodrigo Fonseca, and Tian Guo. Few-shot neural architecture search. *arXiv preprint arXiv:2006.06863*, 2020.
- [40] Barret Zoph and Quoc V Le. Neural architecture search with reinforcement learning. *arXiv preprint arXiv:1611.01578*, 2016.
- [41] Barret Zoph, Vijay Vasudevan, Jonathon Shlens, and Quoc V Le. Learning transferable architectures for scalable image recognition. In *Proceedings of the IEEE conference on computer vision and pattern recognition*, pages 8697–8710, 2018.